US 20050094153A1

(19) **United States**

(12) **Patent Application Publication** (10) **Pub. No.: US 2005/0094153 A1**

Nikoonahad et al. (43) **Pub. Date: May 5, 2005**

(54) **METROLOGY SYSTEM USING OPTICAL PHASE**

(76) Inventors: **Mehrdad Nikoonahad**, Menlo Park, CA (US); **Guoheng Zhao**, Milpitas, CA (US); **Ian Smith**, Los Gatos, CA (US); **Mehdi Vaez-Iravani**, Los Gatos, CA (US)

Correspondence Address:
PARSONS HSUE & DE RUNTZ LLP
655 MONTGOMERY STREET
SUITE 1800
SAN FRANCISCO, CA 94111 (US)

(21) Appl. No.: **11/016,025**

(22) Filed: **Dec. 17, 2004**

Related U.S. Application Data

(63) Continuation of application No. 10/807,603, filed on Mar. 23, 2004, which is a continuation of application No. 09/639,495, filed on Aug. 14, 2000, now Pat. No. 6,710,876.

Publication Classification

(51) **Int. Cl.**[7] **G01B 9/02**

(52) **U.S. Cl.** **356/492**

(57) **ABSTRACT**

Misalignment error between two periodic structures such as two overlay targets placed side-by-side is measured. The two structures are illuminated by coherent radiation and the positive and negative diffraction beams of the input beam by the two structures are detected to discover the optical phase difference between the positive and negative diffraction beams. The misalignment between the two structures may then be ascertained from the phase difference.

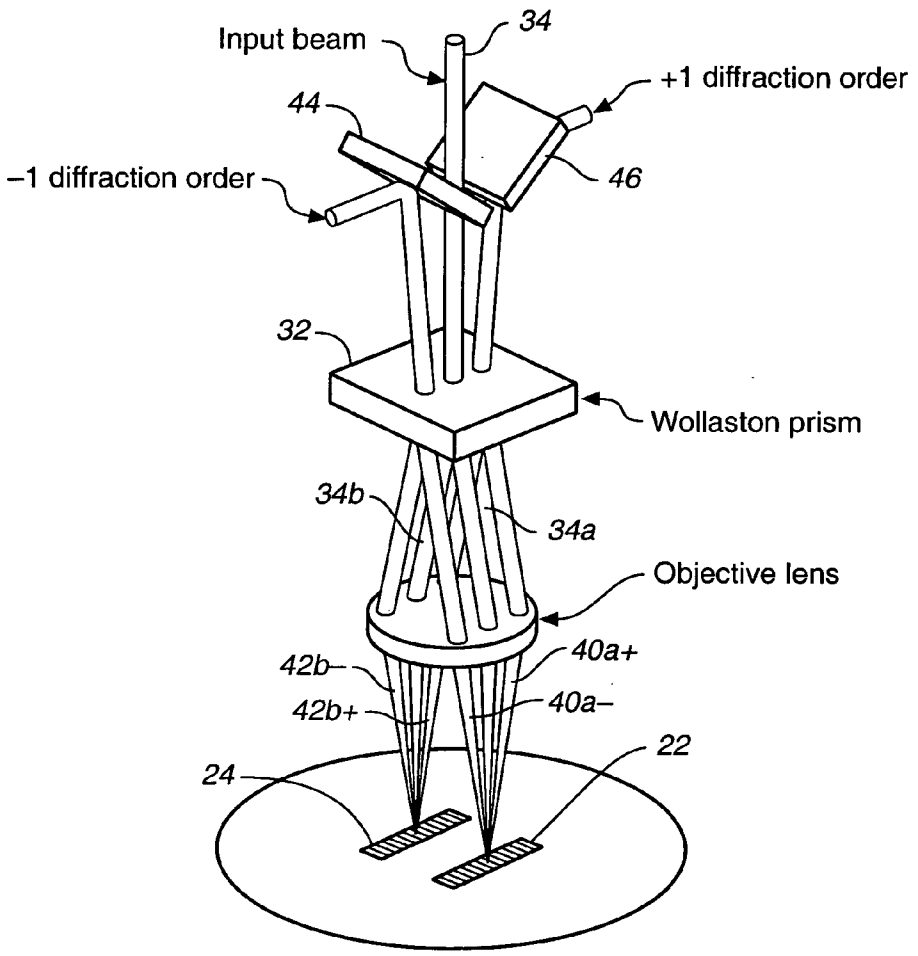

FIG._1

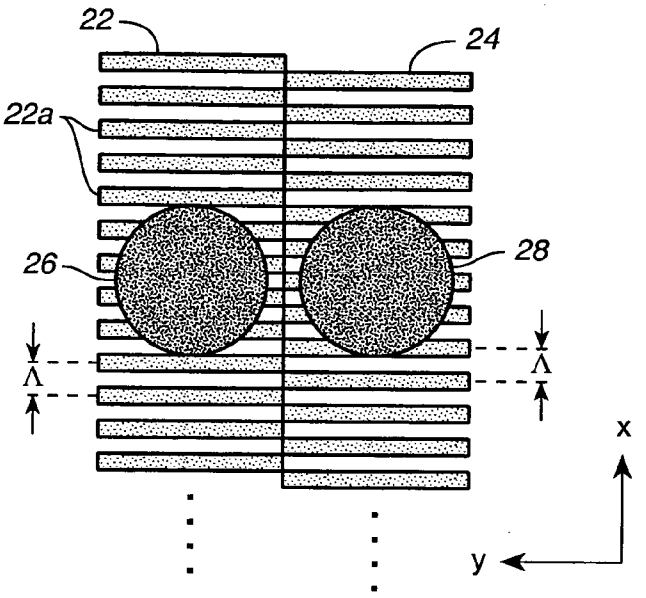

FIG._2

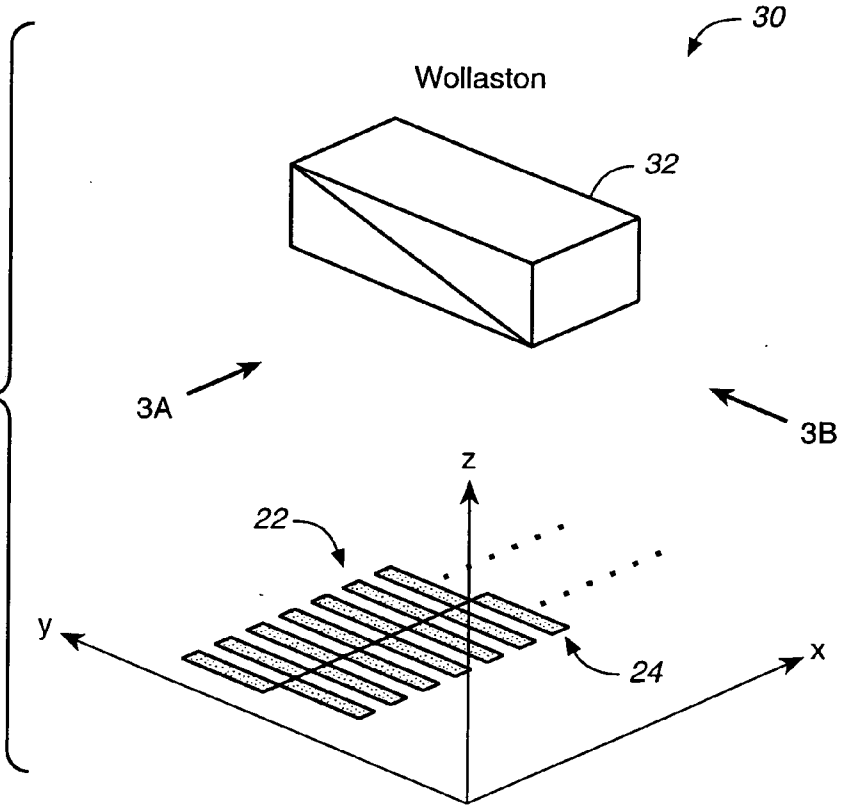

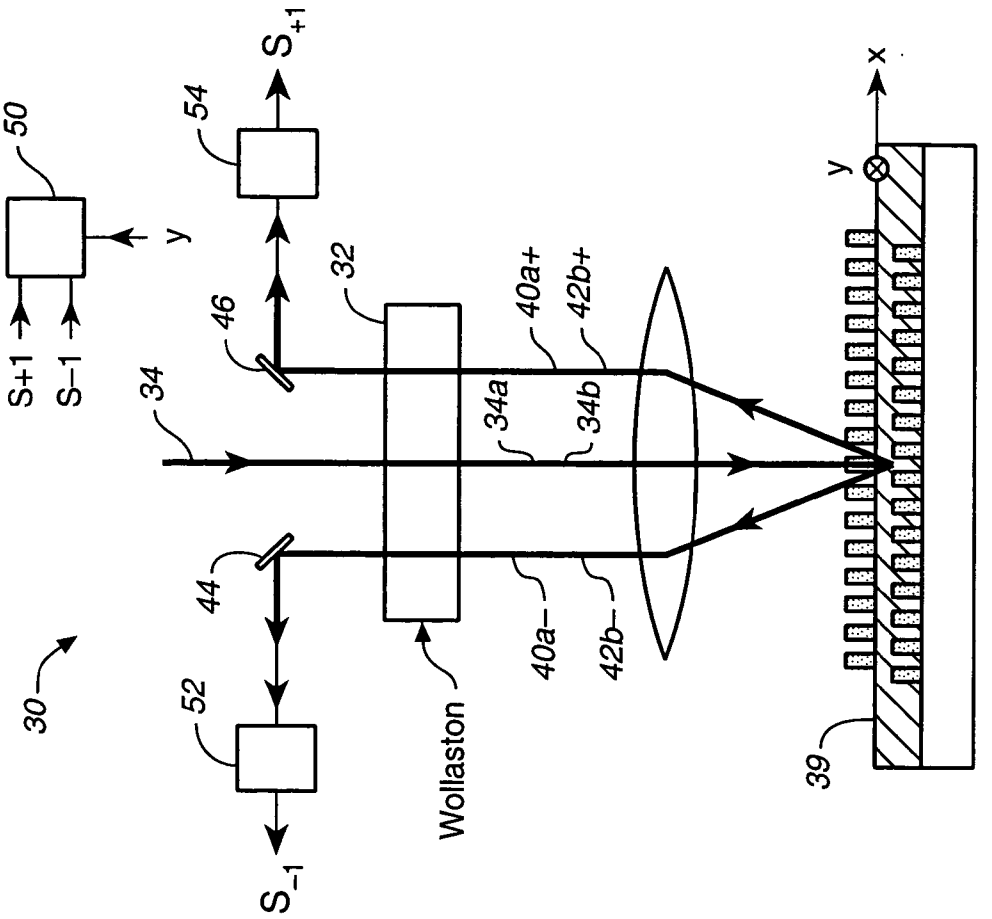
50
S+1
S−1
y
54
S+1
46
32
40a+
42b+
34
34a
34b
44
40a−
42b−
52
S−1
Wollaston
30
x
y
39

FIG._3B

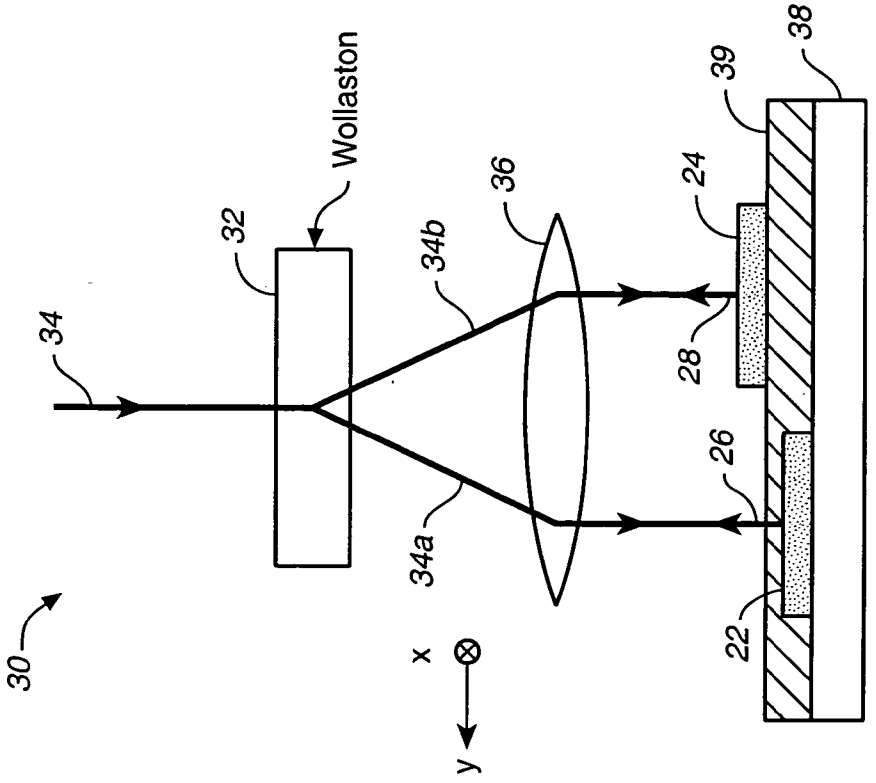
34
32
Wollaston
34b
36
24
39
38
28
26
34a
x
y
22
30

FIG._3A

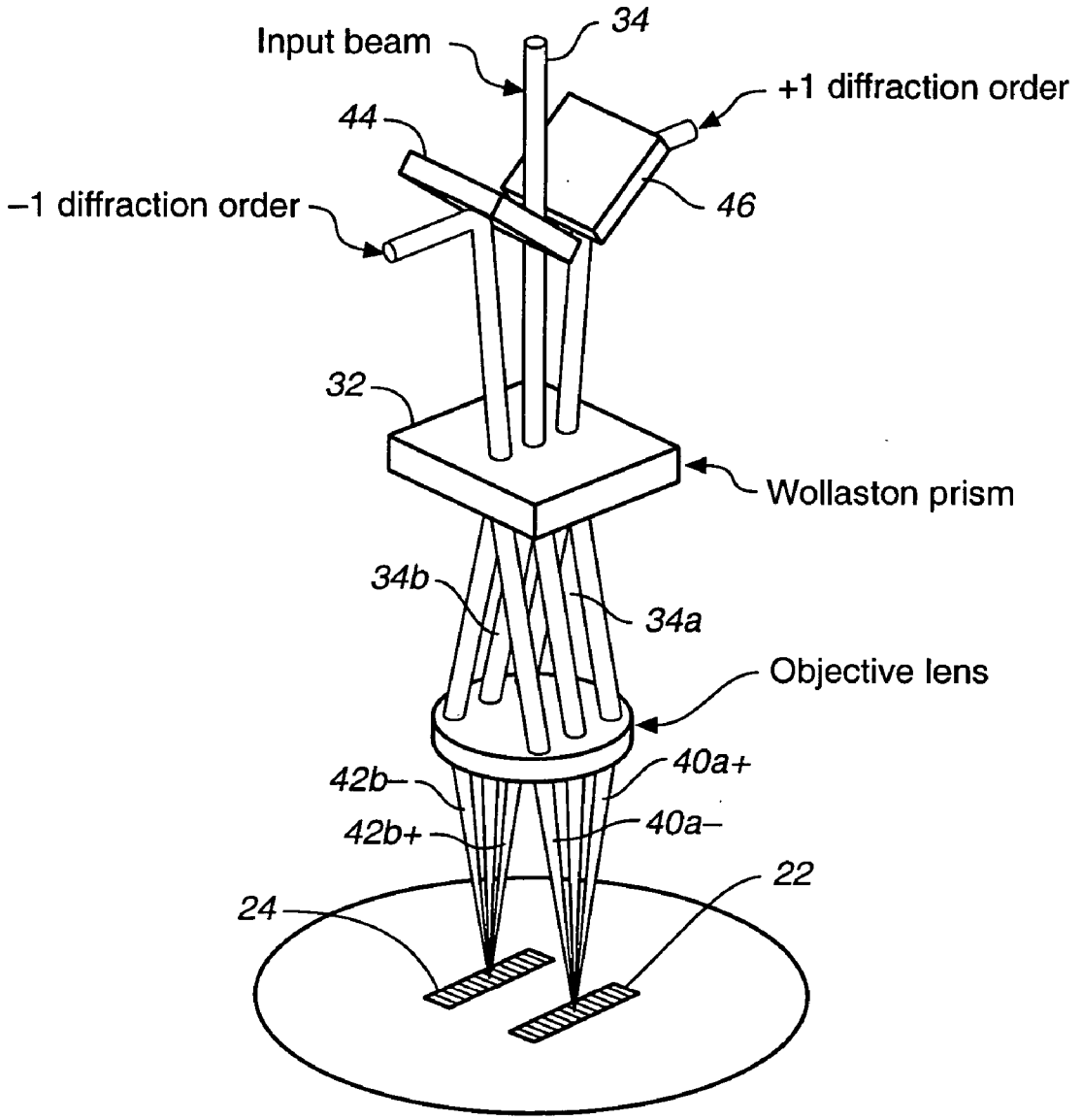
Input beam
34
+1 diffraction order
44
46
−1 diffraction order
32
Wollaston prism
34b
34a
Objective lens
42b−
40a+
42b+
40a−
22
24

FIG._3C

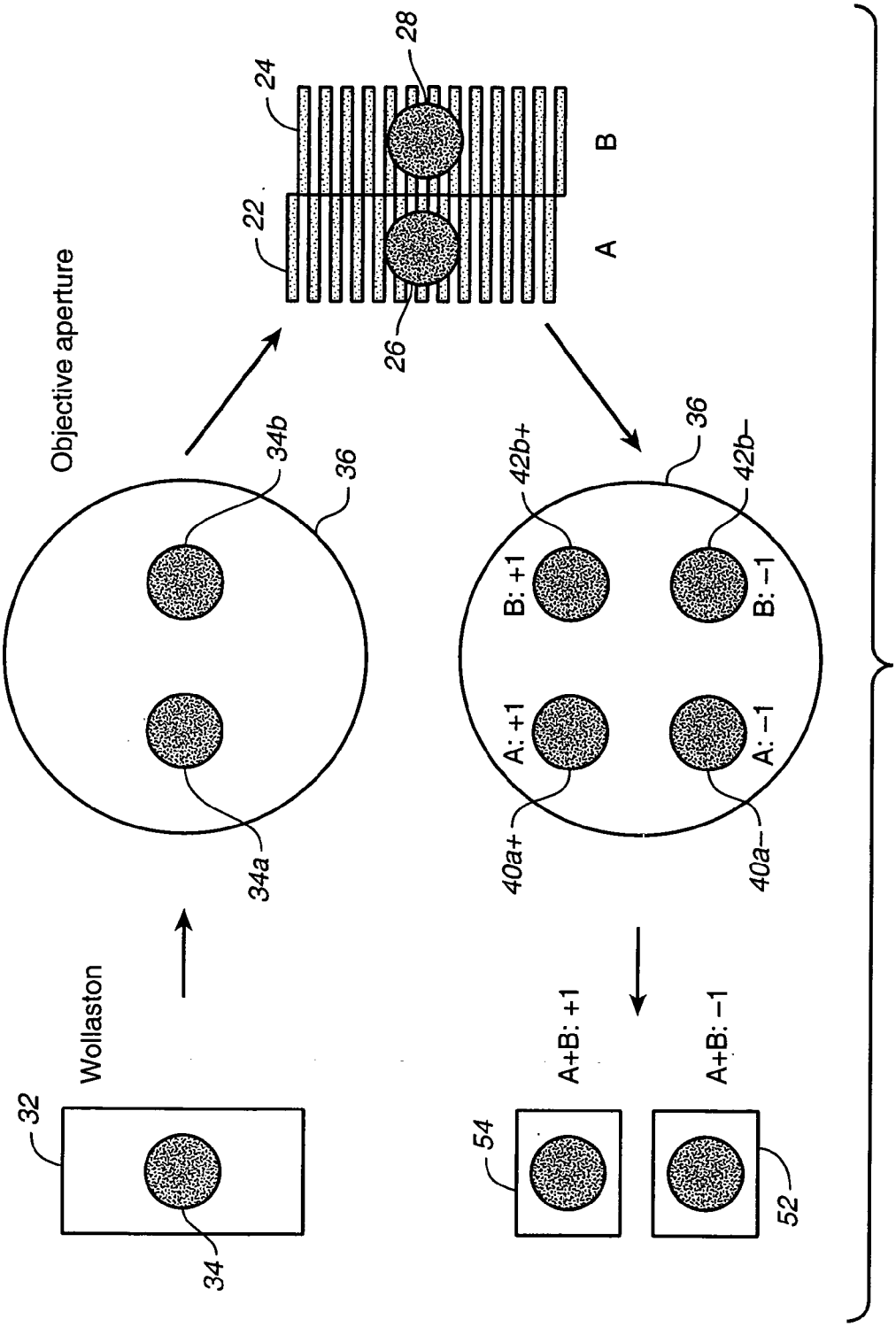
Objective aperture
Wollaston
32
34
34a
34b
36
22
24
26
28
A
B
36
42b+
42b−
B: +1
B: −1
A: +1
A: −1
40a+
40a−
A+B: +1
A+B: −1
54
52

FIG._4

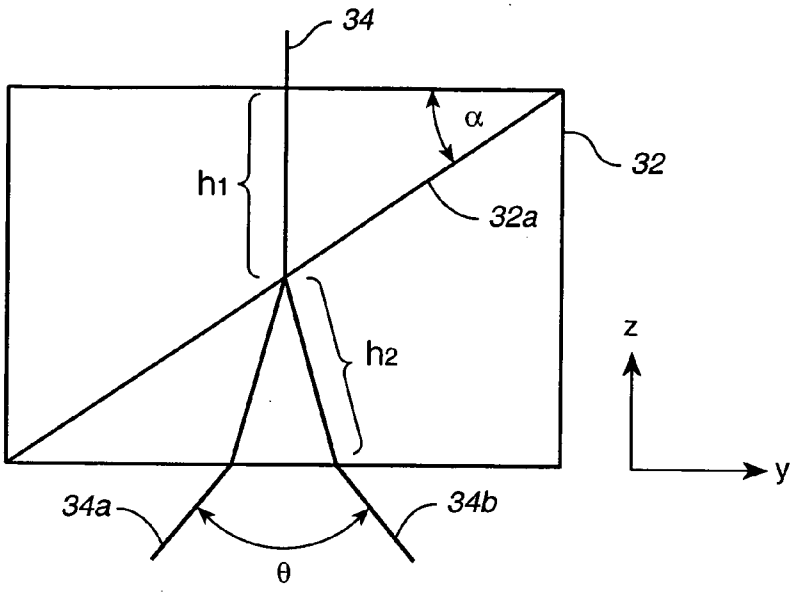
34
α
32
h1
32a
h2
z
y
34a
34b
θ

FIG._5

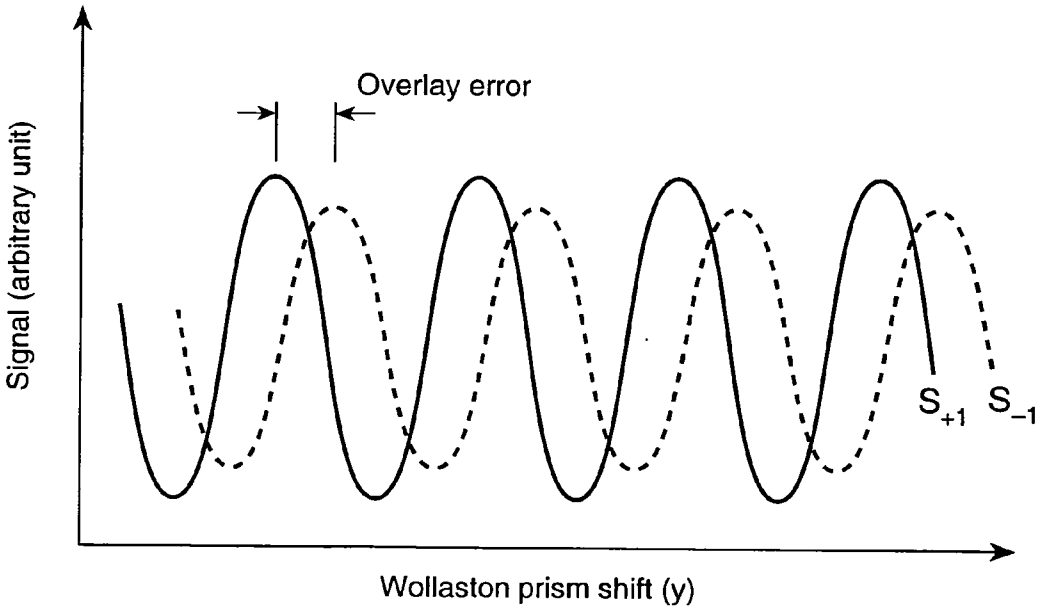
Overlay error
Signal (arbitrary unit)
S+1
S−1
Wollaston prism shift (y)

FIG._6

FIG._7A

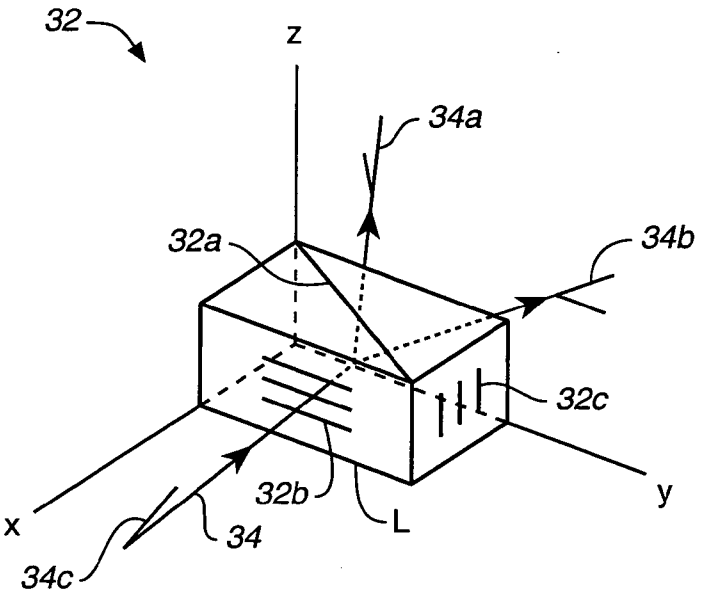
32
z
34a
32a
34b
32c
x
y
32b
L
34
34c

FIG._7B

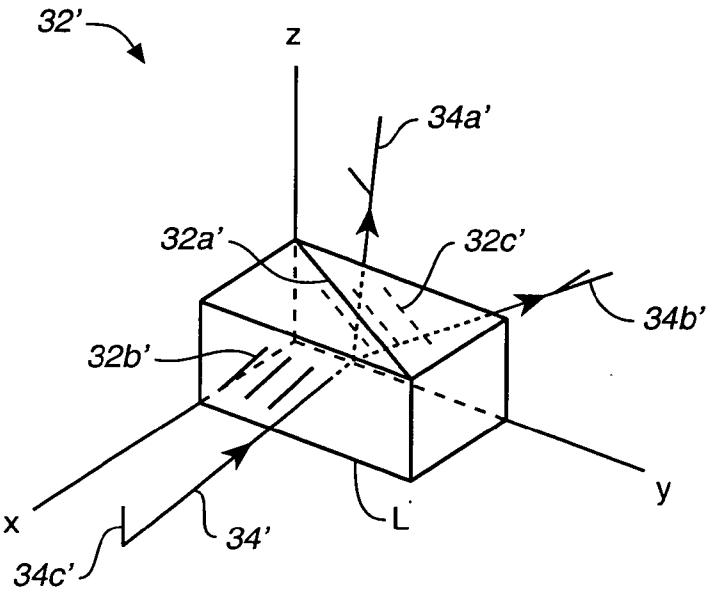
32'
z
34a'
32a'
32c'
34b'
32b'
x
y
L
34'
34c'

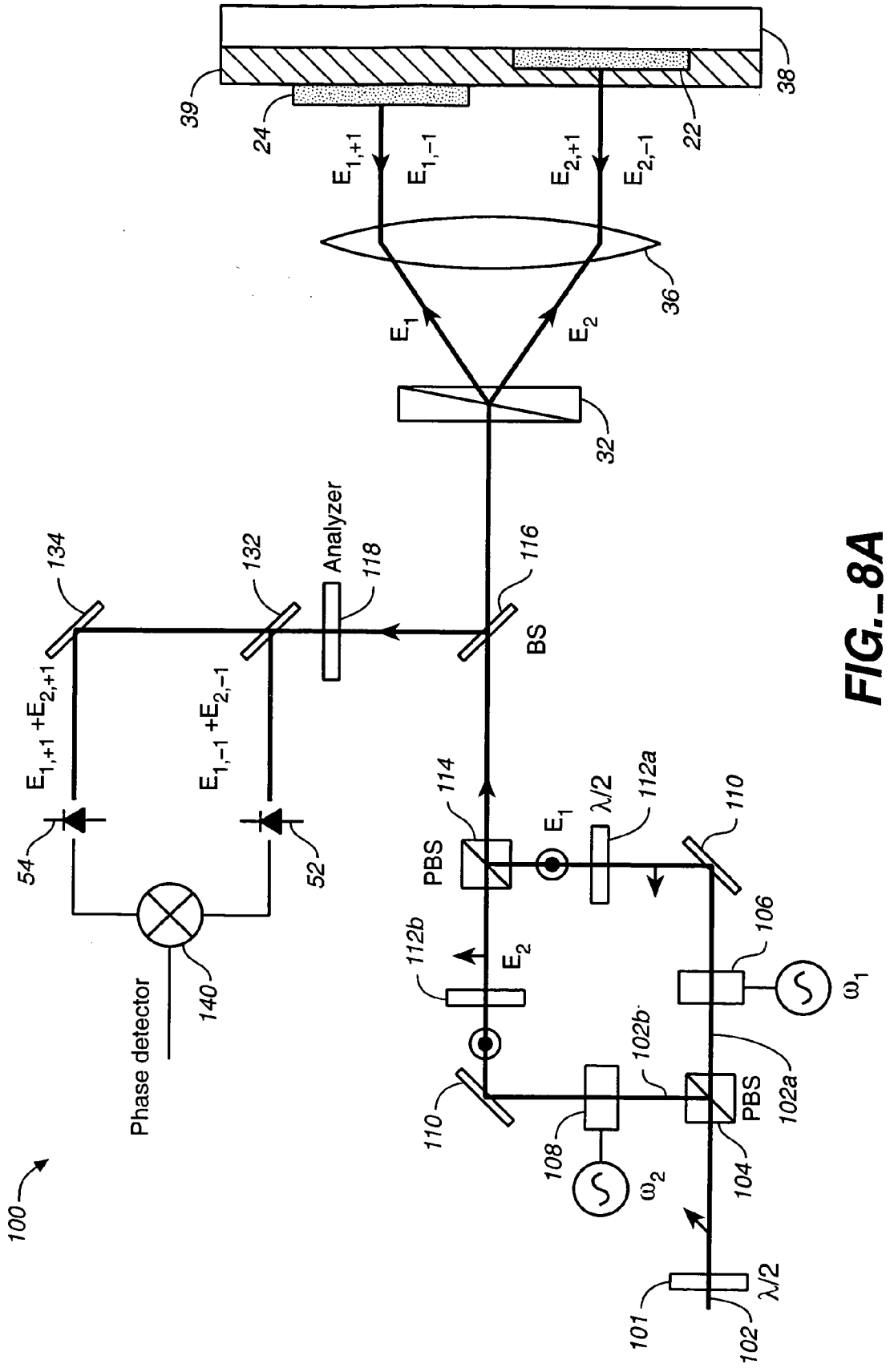
100
101
102
λ/2
104
PBS
102a
102b
106
ω1
108
ω2
110
112a
λ/2
112b
114
PBS
E1
E2
116
BS
118
Analyzer
132
134
E1,+1 +E2,+1
E1,-1 +E2,-1
52
54
140
Phase detector
32
36
E1
E2
E1,+1
E1,-1
E2,+1
E2,-1
22
24
38
39

FIG._8A

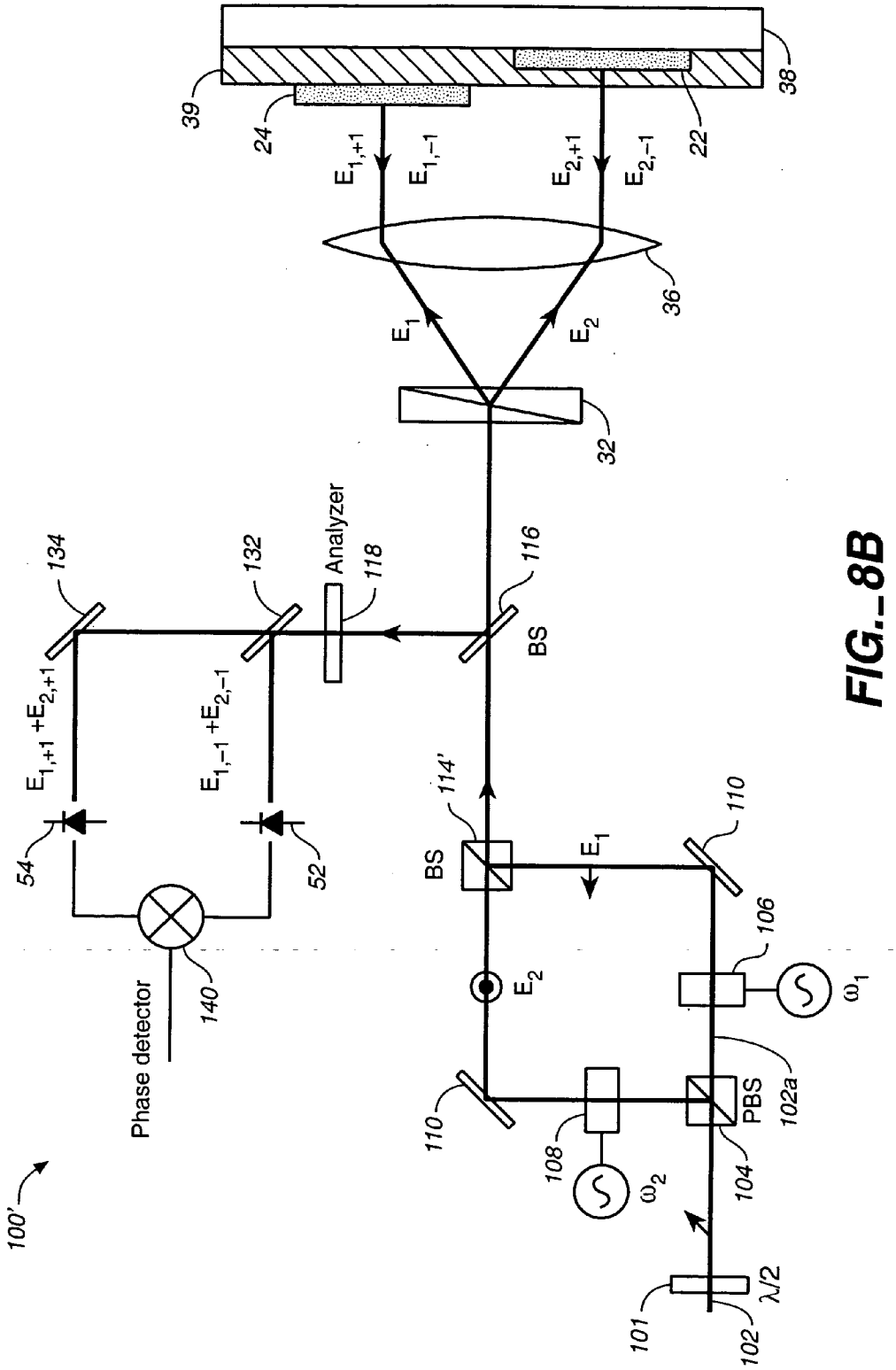
100'
39
24
38
22
$E_{1,+1}$
$E_{1,-1}$
$E_{2,+1}$
$E_{2,-1}$
36
E_1
E_2
32
134
132
Analyzer
118
116
BS
$E_{1,+1}+E_{2,+1}$
$E_{1,-1}+E_{2,-1}$
54
52
114'
BS
E_1
110
E_2
106
ω_1
Phase detector
140
110
108
ω_2
PBS
102a
104
101
$\lambda/2$
102

FIG._8B

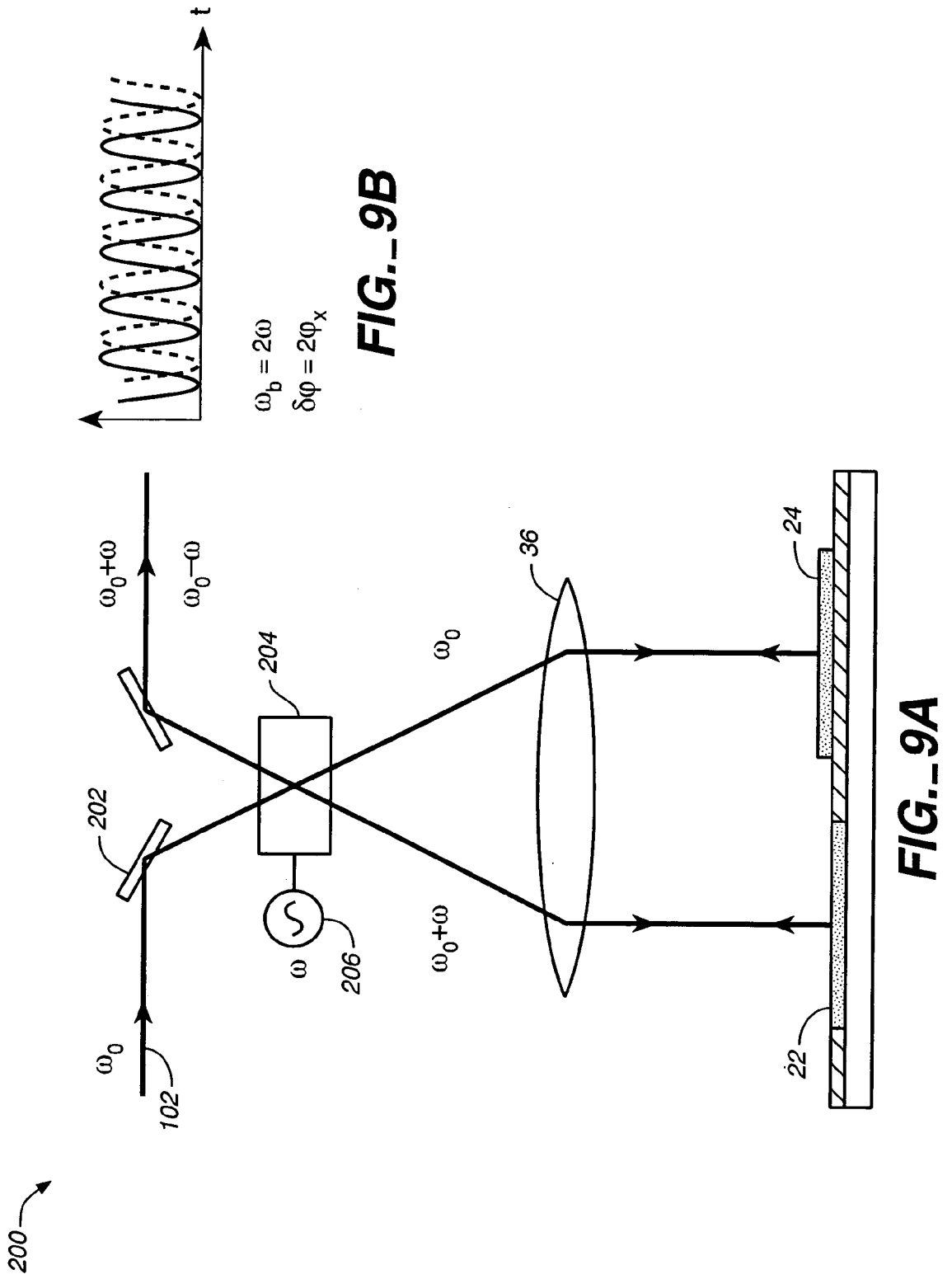
200
ω_0
102
$\omega_0+\omega$
$\omega_0-\omega$
202
204
ω
206
ω_0
$\omega_0+\omega$
36
24
22
t
$\omega_b = 2\omega$
$\delta\varphi = 2\varphi_x$

FIG._9A

FIG._9B

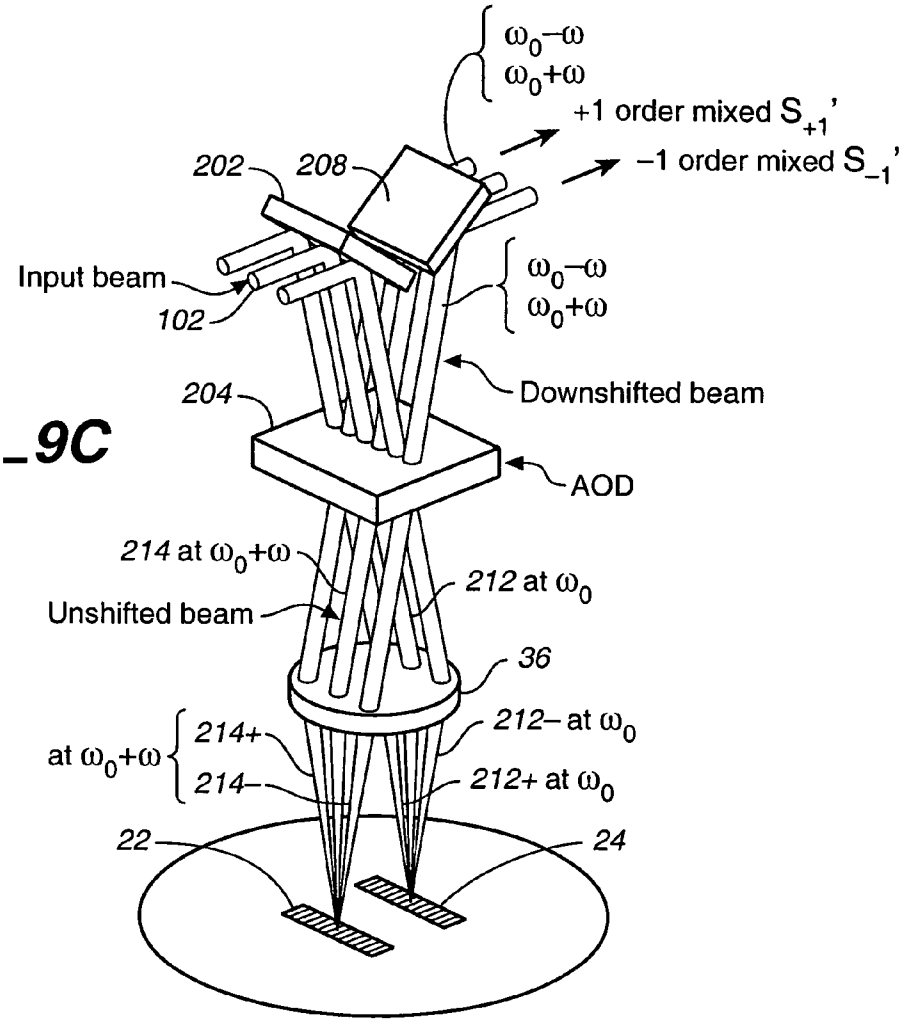
$\omega_0-\omega$
$\omega_0+\omega$
+1 order mixed S_{+1}'
−1 order mixed S_{-1}'
202
208
Input beam
102
$\omega_0-\omega$
$\omega_0+\omega$
204
Downshifted beam
AOD
214 at $\omega_0+\omega$
212 at ω_0
Unshifted beam
36
at $\omega_0+\omega$
214+
214−
212− at ω_0
212+ at ω_0
22
24

FIG._9C

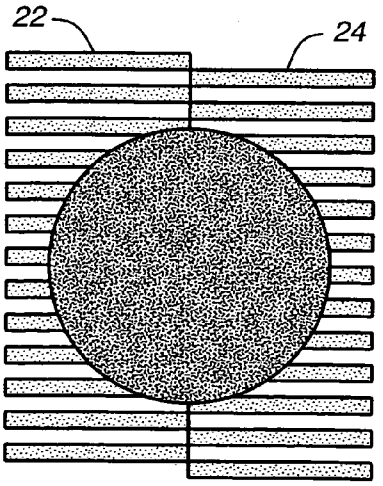
22
24

FIG._10

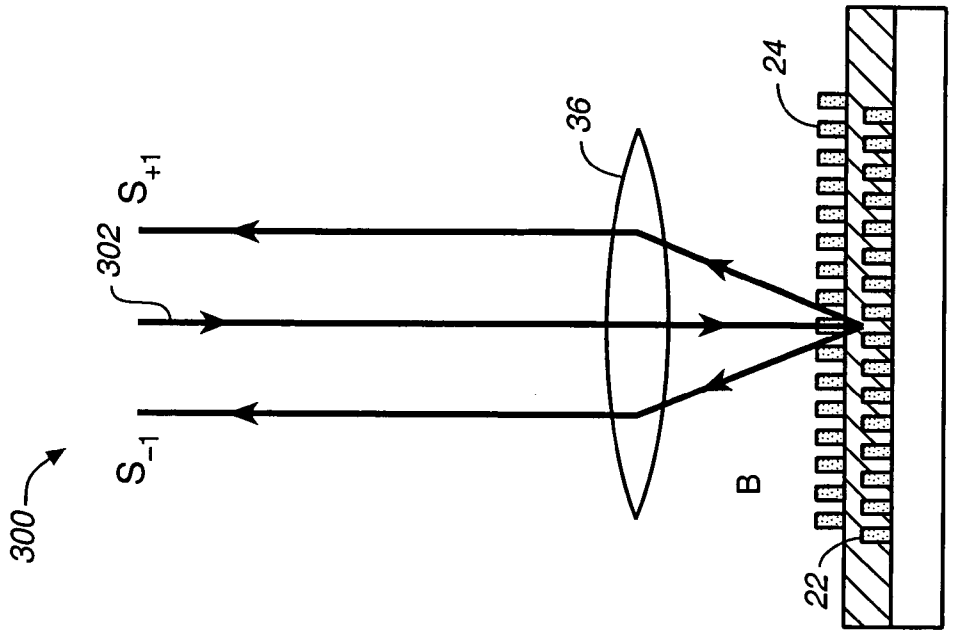

FIG._11B

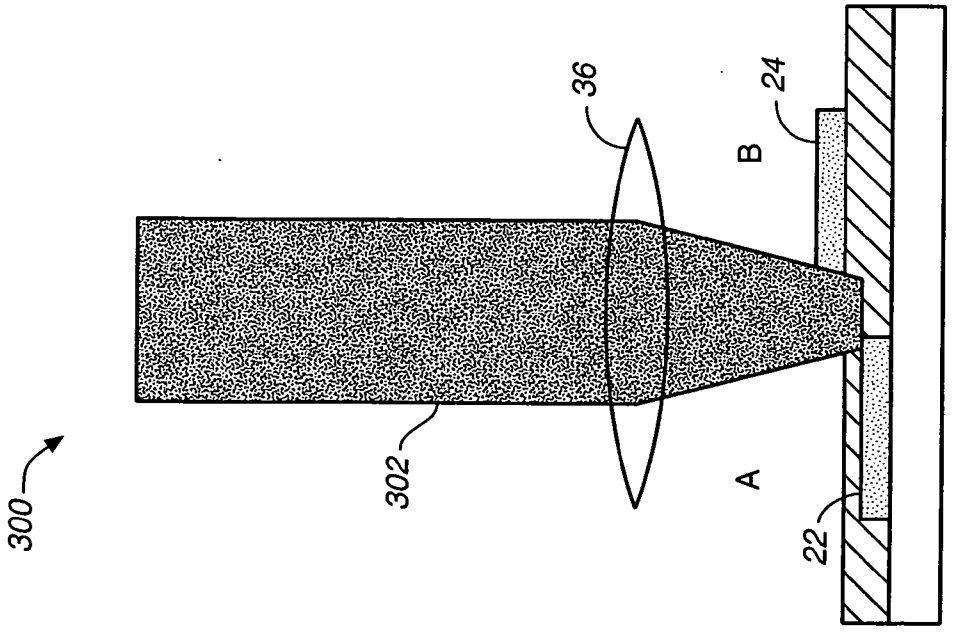

FIG._11A

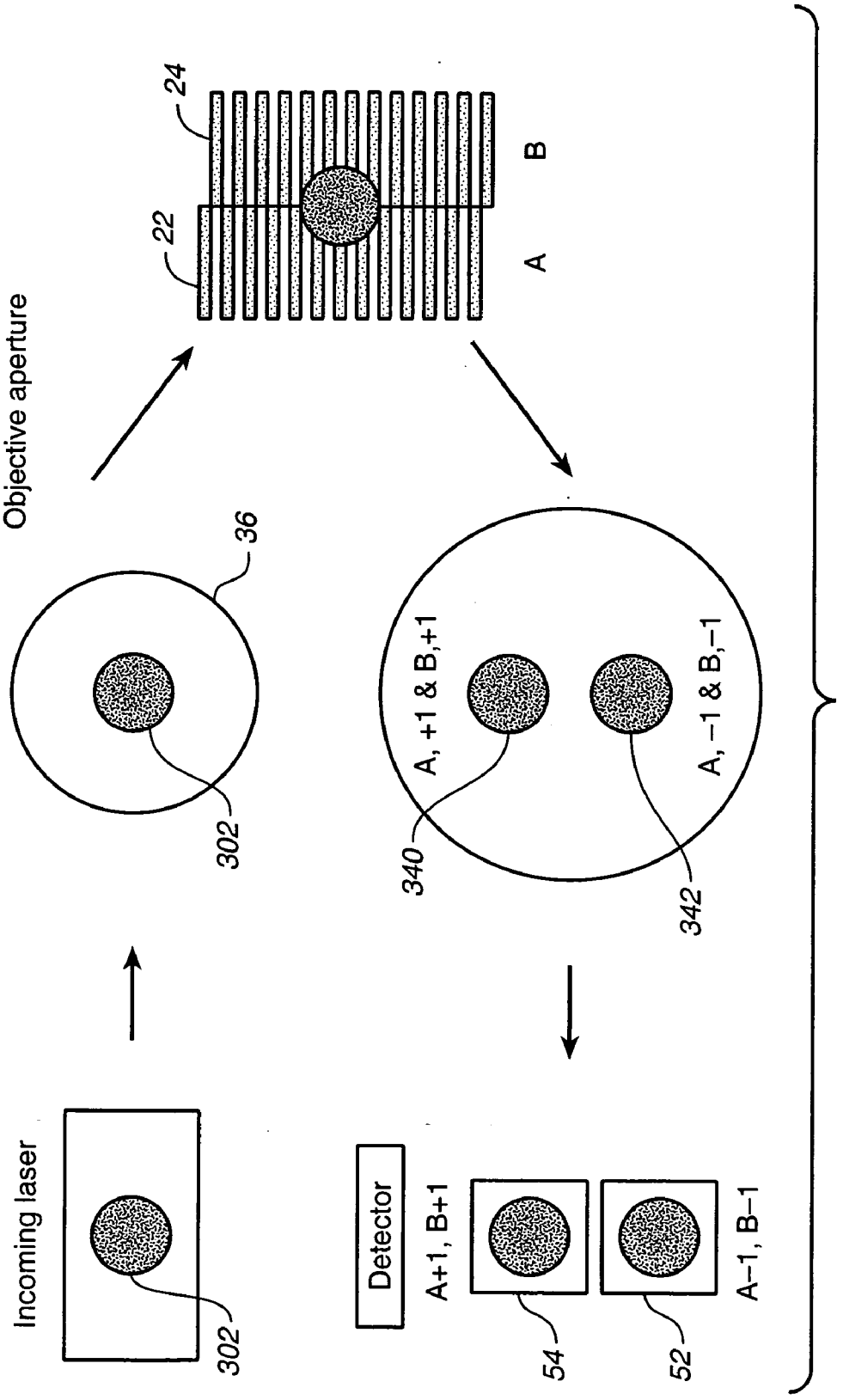
Incoming laser
302
Objective aperture
36
302
24
22
A
B
A, +1 & B,+1
A, −1 & B,−1
340
342
Detector
A+1, B+1
A−1, B−1
54
52

FIG._12

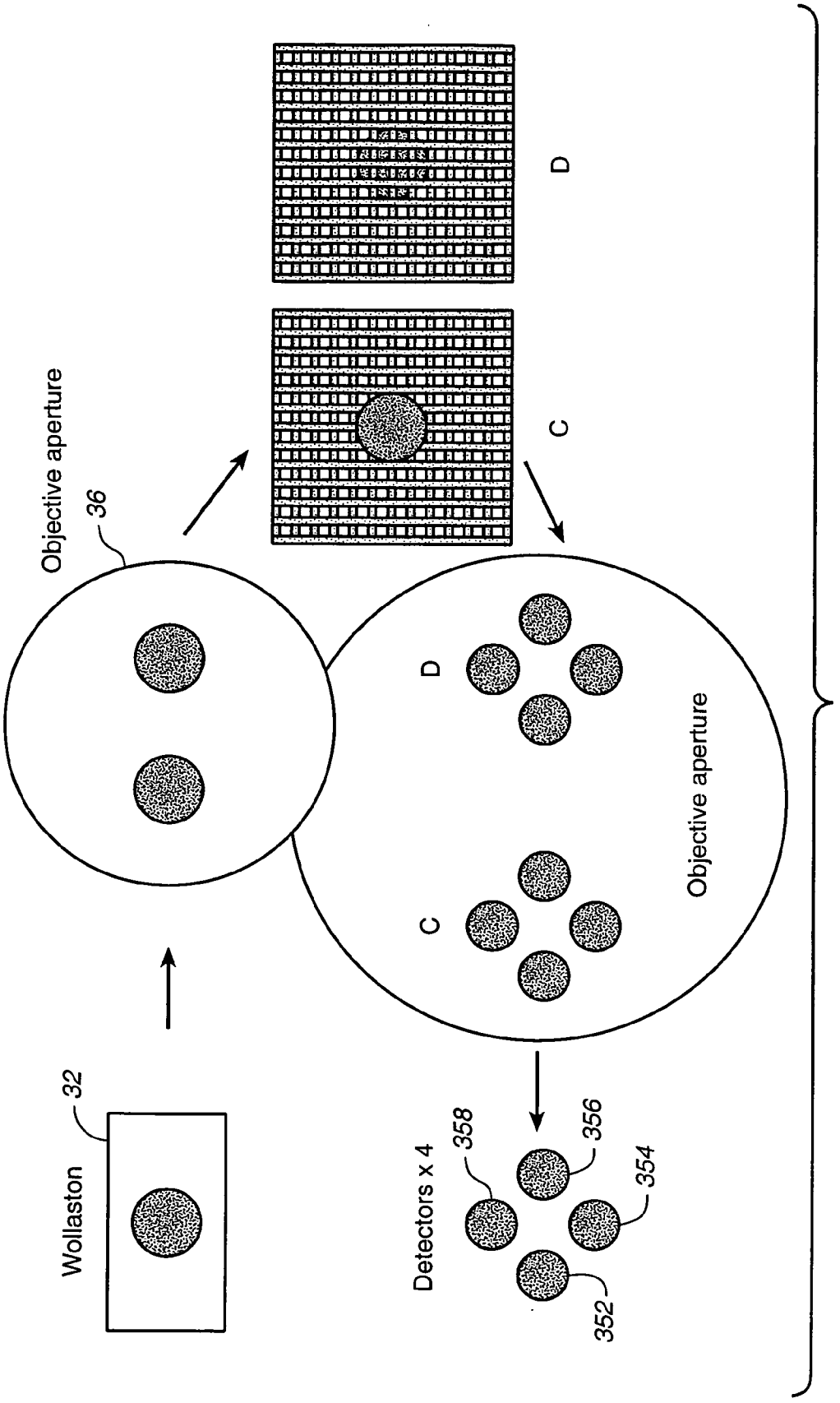
Objective aperture
36
D
C
D
C
Objective aperture
Wollaston
32
Detectors x 4
358
356
354
352

FIG._13

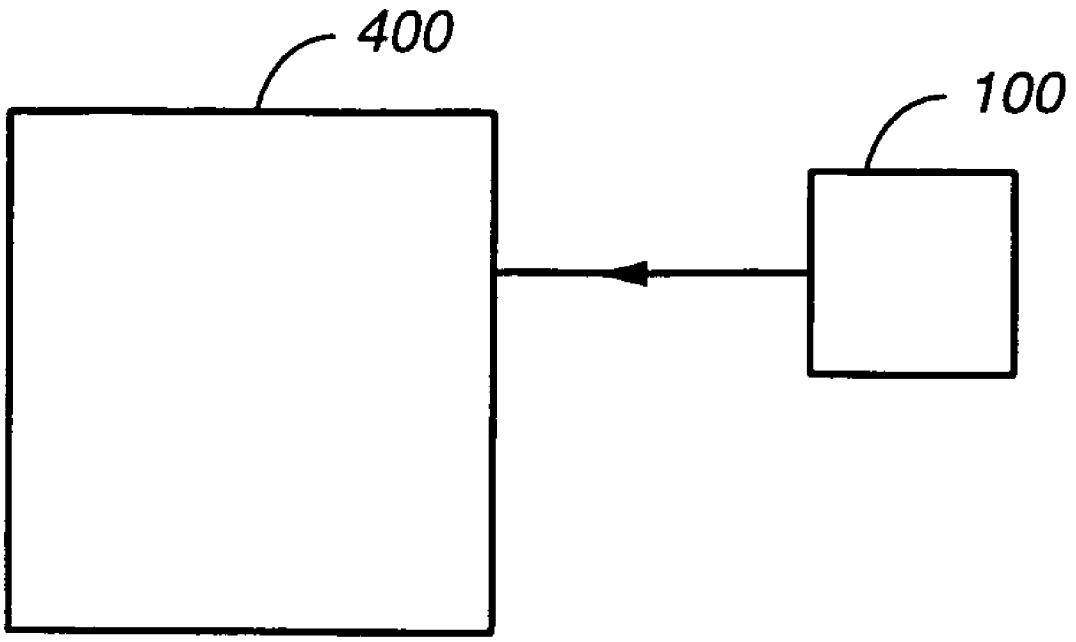

FIG._14

METROLOGY SYSTEM USING OPTICAL PHASE

BACKGROUND OF THE INVENTION

[0001] This invention relates in general to metrology systems for measuring periodic structures such as overlay targets employed in photolithography in a research or production environment, and, in particular, to a metrology system employing optical phase for detecting misalignment of such structures.

[0002] Overlay error measurement requires specially designed marks to be strategically placed at various locations, normally in the street area between dies, on the wafers for each process. The alignment of the two overlay targets from two consecutive processes is measured for a number of locations on the wafer and the overlay error map across the wafer is analyzed to provide feedback for the alignment control of lithography steppers.

[0003] A key process control parameter in the manufacturing of integrated circuits is the measurement of overlay target alignment between successive layers on a semiconductor wafer. If the two overlay targets are misaligned relative to each other, the electronic devices fabricated will malfunction and the semiconductor wafer will need to be reworked or discarded.

[0004] Typically, conventional overlay targets are box-in-box targets and bar-in-bar targets. The box-in-box target typically has a 10 μm inner box and a 20 μm outer box. The outer box is printed on the substrate (or previous process layer) and the inner box is resist printed on the current layer. Overlay error is reported as the mis-position of the inner mark with respect to the outer mark. A bar-in-bar target also has a 10 μm inner target on the current layers and a 20 μm outer target on the previous layers. However, the box edge is replaced with a narrow bar 2 μm wide. The box-in-box targets are more compact; however, the bar-in-bar targets provide better measurement performance. Overlay targets may comprise grating structures on top of the wafer or etched into the surface of the wafer. For example, one overlay target may be formed by etching into the wafer while another adjacent overlay target may be a photoresist layer at a higher elevation over the wafer.

[0005] Conventional systems for detecting overlay target misalignment typically employs an electronic camera that images the "box-in-box target." The accuracy of the conventional system is limited by the accuracy of the line profiles in the target, by aberrations in the illumination and imaging optics and by the image sampling in the camera. Such methods are complex and they require full imaging optics. Vibration isolation is also required and it may be difficult to integrate such systems into process equipment.

[0006] An improvement to the conventional method is described in U.S. Pat. No. 6,023,338. This patent discloses a method where two overlay target structures are placed next to each other and two radiation beams are scanned in two separate paths across portions of both structures. The intensity of the radiation reflected along both paths are detected and processed to calculate any offset between the two structures.

[0007] While the above-described improved method may be useful for some applications, it requires beams to be scanned across periodic structures such as overlay targets. It is desirable to develop an improved system with better performance and simplified scanning characteristics.

SUMMARY OF THE INVENTION

[0008] This invention is based on the observation that by utilizing optical phase detection, high sensitivity for detecting misalignment of periodic structures can be achieved. Thus, two periodic structures such as overlay targets are placed side-by-side so that they are periodic substantially along the same direction, where portions of both structures are illuminated by coherent radiation. The size(s) of the beam(s) illuminating portions of the structures are large enough to generate diffraction signals by the structures. These diffraction signals are caused to interfere leading to the detection of optical phase which is a measurement of the misalignment between the, structures. The misalignment may then be used to control lithographic instruments such as a lithographic stepper or to determine whether or not the patterns of the structures are correctly placed and will yield functional devices.

[0009] When the paths of radiation traveling between the radiation source, the structures and detectors are close together, the phase sensitive detection is less sensitive to environmental factors such as vibration and thermal drifts. Since the system employs larger spot illumination, the optics of the system are less sensitive to focus accuracy. The system is compact and readily integratable with process equipment. Due to the enhanced sensitivity compared to conventional systems, the system is able to detect misalignment of periodic structures that are low contrast.

BRIEF DESCRIPTION OF THE DRAWINGS

[0010] **FIG. 1** is a top view of two overlay targets placed next to each other that are illuminated by two corresponding radiation beams to illustrate the invention.

[0011] **FIG. 2** is a perspective view of two overlay targets placed side-by-side and a Wollaston prism useful for illustrating the invention.

[0012] **FIGS. 3A and 3B** are side views from different angles of an overlay target metrology system illustrating an embodiment of the invention. **FIG. 3C** is a perspective view of the system of **FIGS. 3A and 3B**.

[0013] **FIG. 4** is a flow diagram illustrating cross-sectional light distributions at various positions in the paths of radiation beams in the system of **FIGS. 3A and 3B**.

[0014] **FIG. 5** is a schematic view of the Wollaston prism of **FIGS. 3A and 3B** illustrating its function in dividing a beam of radiation into two beams.

[0015] **FIG. 6** is a graphical plot of output signals from the detectors of **FIGS. 3A and 3B** to illustrate a method for obtaining offset or misalignment information between the overlay targets from the detector outputs.

[0016] **FIG. 7A** is a schematic view of a conventional Wollaston prism dividing an input polarized beam into two polarized beams useful for illustrating the invention.

[0017] **FIG. 7B** is a schematic view of a modified Wollaston prism dividing an input polarized beam into two, useful for illustrating the invention.

[0018] **FIG. 8A** is a partially schematic and partially cross-sectional view of a dual heterodyne differential phase metrology system for measuring misalignment of two adjacent overlay targets to illustrate a preferred embodiment of the invention.

[0019] **FIG. 8B** is a partially schematic and partially cross-sectional view of a dual heterodyne differential phase metrology system for measuring misalignment of two adjacent overlay targets to illustrate an embodiment of the invention similar to that of **FIG. 8A** in many respects.

[0020] **FIG. 9A** is a cross-sectional view of a metrology system for measuring misalignment of overlay targets to illustrate another embodiment of the invention.

[0021] **FIG. 9B** is a graphical plot of the output signals from the metrology system of **FIG. 9A**.

[0022] **FIG. 9C** is a perspective view of the system of **FIGS. 9A and 91**.

[0023] **FIG. 10** is a top view of two overlay targets placed adjacent to each other illuminated by a single beam of radiation to illustrate yet another embodiment of the invention.

[0024] **FIGS. 11A and 11B** are two side views from different angles of a metrology system where a single beam of radiation is employed to illuminate two overlay targets for detecting misalignment illustrating yet another embodiment of the invention.

[0025] **FIG. 12** is a flow diagram illustrating the cross-sectional light distributions at various positions of radiation beams in the system of **FIGS. 11A and 11B**.

[0026] **FIG. 13** is a flow diagram illustrating the cross-sectional light distributions at various positions of radiation beams in the system of **FIGS. 3A and 3B** where the two overlay targets are periodic in two orthogonal directions.

[0027] **FIG. 14** is a block diagram illustrating a lithographical instrument in combination with a metrology system for measuring misalignment of overlay targets to illustrate still another embodiment of the invention.

[0028] For simplicity of description, identical components are labeled by the same numerals in this application.

DETAILED DESCRIPTION OF THE EMBODIMENTS

[0029] **FIG. 1** is a top view of two periodic structures **22, 24** such as overlay targets, placed side-by-side, where both structures are illuminated by a beam of radiation having a round cross-section as shown in **FIG. 1**. Preferably both structures **22, 24** have the same period A, and are preferably aligned so that they are periodic substantially along the same line of direction X in the XY coordinate system. The two illuminated spots **26, 28** are preferably aligned with the centers of the spots substantially aligned along the Y axis. This can be achieved, for example, by aligning the two spots with two markers on one of the overlay target structures to correctly position the two spots. The size of spot **26** along the X axis is such that its dimension along the X axis is at least equal to or greater than the period Λ (more typically equal to or greater than several periods Λ's) in order for a diffracted signal to be generated by illuminating structure **22** at spot **26**. Preferably, spot **26** would span a number of grating lines **22***a* of structure **22**. The same can be said of spot **28** with respect to the period A and other features of structure **24**.

[0030] A metrology system **30** for generating the two illuminated spots **26, 28** on the two corresponding structures is illustrated in **FIG. 2**. As shown in **FIG. 2**, a beam of radiation (not shown) may be split by means of a Wollaston prism **32** to illuminate the two structures **22** and **24**. As shown in **FIG. 2**, the Wollaston prism is located above the two structures at a predetermined z height above the structures.

[0031] **FIGS. 3A and 3B** are side views of the metrology system **30** of **FIG. 2** in directions along the arrows **3**A, **3**B in **FIG. 2**, respectively. **FIG. 3C** is a perspective view of system **30**. As shown in these figures, a beam of radiation **34** is split by prism **32** into two beams **34***a*, **34***b* in the Y direction. These two beams are collected by lens **36** towards two overlay target structures **22, 24** which are placed side-by-side above a substrate **38** such as a silicon wafer. Beam **34***a* illuminates spot **26** on structure **22** and beam **34***b* illuminates spot **28** of structure **24**. Beam **34***a* is diffracted by structure **22**. The zeroth-order diffraction retraces the original path of beam **34***a* and through prism **32**. The first order diffraction **40***a*-and **40***a*+from structure **22** of beam **34***a* are collected by lens **36** towards prism **32** and reflected by mirrors **44** and **46** towards two detectors **52, 54** as shown in **FIG. 3B**. Similarly, the zeroth-order diffracted signal from structure **24** of beam **34***b* retraces the original path of beam **34***b*. The first order diffracted signals **42***b*+ and **42***b*− are collected by lens **36** through prism **32** to the two detectors **52, 54**. The relative positions of the various beams of radiation in **FIGS. 3A and 3B** are shown more clearly in the flow diagram of **FIG. 4**. The outputs of detectors **52, 54** are S_{-1} and S_{+1}, respectively, as shown in **FIG. 3B**. As shown in **FIG. 4**, the input beam **34** is applied to Wollaston prism **32** which splits or divides the beam into two beams **34***a*, **34***b* when it reaches the objective **36**. After passing through the objective, the two beams **34***a*, **34***b* illuminate, respectively, spots **26, 28** of structures **22, 24**. To simplify the figures, the zeroth-order diffracted signal from the two structures have been omitted from **FIG. 4**. The positive and negative diffracted signals **40***a*+ and **40***a*− are collected by lens **36**. Similarly, the positive and negative first diffraction signal **42***b*+ and **42***b*− are collected by lens **36** towards prism **32**. Prism **32** combines beams **40***a*+ and **42***b*+ from the two spots **26, 28** into one beam towards detector **54**. The input beam **34** is coherent so that beams **34***a*, **34***b* are coherent after passing prism **32**. Therefore, the positive first order diffraction **40***a*+ and **42***b*+ are also coherent. They would, therefore, interfere when combined by prism **32** and at detector **54**. Similarly, the negative first order diffracted signals **40***a*− and **42***b*− are combined by prism **32** and interfere at the prism and at the detector **52**. The phase difference between the outputs of the two detectors **52, 54** is determined. This phase difference indicates the phase difference between beams **40***a*+, **42***b*+ and that between the pair of beams **40***a*− and **42***b*−, and provides information concerning misalignment between the two structures **22, 24**. The two output signals S_{+1} and S_{-1} are shown in Equations 1 and 2 below:

$$S_{+1} \propto \{\eta_{+1}{}^{a}+\eta_{+1}{}^{b}+2\sqrt{\eta_{+1}{}^{a}\eta_{+1}{}^{b}}\cos(\phi_{+1}+\phi_{w}+\phi_{z}+\phi_{x})\} \quad (1)$$

$$S_{-1} \propto \{\eta_{-1}{}^{a}+\eta_{-1}{}^{b}+2\sqrt{\eta_{-1}{}^{a}\eta_{-1}{}^{b}}\cos(\phi_{-1}+\phi_{w}+\phi_{z}-\phi_{x})\} \quad (2)$$

[0032] In the equations (1) and (2) above, η_{+1}^{a} is the diffraction efficiency of the diffracted signal **40***a*+ from interaction between structure **22** and beam **34***a* at spot **26**, η_{+1}^{b}, the diffraction efficiency of the +1 diffracted signal **42***b*+ from interaction between structure **24** and beam **34***b* at spot **28**, η_{-1}^{a} the diffraction efficiency of the diffracted signal **40***a*− from interaction between structure **22** and beam **34***a* at spot **26**, and η_{-1}^{b} the diffraction efficiency of the −1 diffracted signal **42***b*− from interaction between structure **24** and beam **34***b* at spot **28**. The phase terms ϕ_{+1} and ϕ_{-1} are residual phase differences due to the grating property difference and are defined by the equations below:

$$\phi_{+1}=\phi_{+1}^{a}-\phi_{+1}^{b};$$

$$\phi_{-1}=\phi_{-1}^{a}-\phi_{-1}^{b}$$

[0033] where ϕ_{+1}^{a} and ϕ_{-1}^{a} are the phase terms in the positive and negative diffracted signals, where such phase terms depend on the material and other properties of structure **22**; and ϕ_{+1}^{b} and ϕ_{-1}^{b}, are the phase terms in the positive and negative diffracted signals, where such phase terms depend on the material and other properties of structure **24**: The two phase differences ϕ_{+1} and ϕ_{-1} are identical for +1 and −1 orders if the grating profile is symmetric. The term ϕ_x is the phase difference caused by any misalignment Δx between the two periodic structures **22**, **24** as set forth in equation (3) below. The amount of this phase shift is readily determined from the shifting theorem of Fourier transform. The grating with period Λ in frequency domain has a spatial frequency at $1/\Lambda$. A phase shift Δx in space translates into $2\pi(1/\Lambda)\Delta\chi$ phase shift in frequency domain, direcily predicted by shifting theorem. The term ϕ_x is the phase difference between the two detector outputs caused by the height difference Δz between the two structures **22**, **24** as shown in equation (4) below. The term ϕ_w is the phase difference between the two detector outputs caused by phase shift induced by the Wollaston prism **32** as shown in equation (5) below.

$$\phi_x = \frac{2\pi}{\Lambda}\Delta x \tag{3}$$

$$\phi_z = \frac{2\pi}{\lambda}n\Delta z \tag{4}$$

$$\phi_w = \frac{2\pi}{\lambda}(n_o - n_e)\Delta h \tag{5}$$

[0034] where Λ is the grating period of structures **22**, **24**; n the average index of refraction of material **39**; n_o, n_e the indices of refraction for the ordinary and extraordinary rays of the prism **32**; λ the wavelength of beam **34**, and Δh is defined below.

[0035] **FIG. 5** is a schematic view of the Wollaston prism **32** of **FIGS. 3A, 3B** illustrating its function in dividing a beam of radiation into two beams and the phase shift introduced by the prism. As shown in **FIG. 5**, beam **34** is split by prism **32** into two beams **34***a*, **34***b* with an angle θ in between them, where θ is given by equation (6) below. The phase difference caused by prism **32** between the two detector outputs S_{+1} and S_{-1} is given by equation (7) below, where n_o and n_e are the refractive indices of prism **32** in the ordinary and in the extraordinary directions of the prism. The term Δh in equation (5) above is the optical path length difference between h1 (the optical path length of beam **34** in prism **32** before reaching the optical interface **32***a*) and **112** (the optical path length of beams **34***a* and **34***b* through the prism after the interface **32***a*). When prism **32** is moved along the y direction relative to beam **34**, beam **34** will reach the interface **32***a* of prism **32** at a different position, thereby changing the optical-path lengths h1, h2 and also changing the quantity Δh. Ah is proportional to the distance y traveled by prism **32** as set forth below:

$$\Delta h=2y\alpha$$

[0036] where α is the angle the optical interface **32***a* makes with the sides of the prism through which the beams **34**, **34***a*, **34***b* pass as shown in **FIG. 5**, so that equation (5) becomes equation (7) below.

$$\theta=2\alpha(n_o-n_e) \tag{6}$$

$$\varphi_w = \frac{2\pi}{\lambda}2\alpha(n_o - n_e)y = \frac{2\pi}{\lambda}y\theta \tag{7}$$

[0037] where the origin of the Y axis is at the position where $h_1=h_2$. The separation δy between two spots on target is given by:

$$\delta y = 2f\tan\left(\frac{\theta}{2}\right) \tag{8}$$

[0038] where f is the objective focal length. For small angle θ, an approximation of this formula becomes:

$$\delta y=f\theta$$

[0039] Thus, by moving prism **32** along the y axis and thereby changing the value of y, the phase term ϕ_w changes as a function of y, which, in turn, causes the two detector outputs S_{+1} and S_{-1} to also change as a function of the displacement y of prism **32** along the y axis, as illustrated in **FIG. 6**. As noted above, if the grating profiles of structures **22**, **24** are symmetric, ϕ_{+1} and ϕ_{-1} are identical. The phase term ϕ_z is the same for both detector outputs. Therefore, the phase difference between the two detector outputs S_{+1} and S_{-1} in **FIG. 6** is caused only by the overlay target error in equation (3). In other words, the phase difference $\Delta\phi$ between the two detector outputs is given by $2\phi_x$ as indicated in equation (9) below:

$$\Delta\phi=2\phi_x \tag{9}$$

[0040] wherein the phase difference between detector signals S_{+1} and S_{-1}: twice overlay error. Therefore, by measuring the phase difference between the two detector outputs at different displacement values of y as indicated in **FIG. 6**, the misalignment Ax between the two structures **22**, **24** can be determined from equations (3) and (9) and the grating period of structures **22**, **24**. This may be performed by a processing device **50** in **FIG. 3B**, where the device may simply be a microprocessor, or programmable logic or any other suitable processing device which can compute the misalignment Δx from the two outputs S_{+1} and S_{-1}.

[0041] As a practical matter, normally Wollaston prisms are designed such that the optical axis **32***b* (shown in a YZ plane as shown in **FIG. 7A**) is parallel to the length L in one

half and the optical axis **32***c* (shown in an XZ plane as shown in **FIG. 7A**) is perpendicular to the length in the other half of the prism, where the two halves are separated by optical interface **32***a*, so that the two beams **34***a*, **34***b* will be either parallel polarized or orthogonally polarized with respect to the grating fingers of structures **22**, **24**. The two different polarizations of the two beams have different diffraction efficiencies. This can cause an imbalance in amplitude between the two outputs S_{-1} and S_{+1}. This tends to limit the sensitivity of system **30** for a given bandwidth. It is possible to overcome this problem by rotating the prism by 45°, so that the polarization direction **34***c* is at 45° to the optical axis **32***b*, and so that the polarizations of the two beams **34***a*, **34***b* will be at +45 and −45° respectively with respect to the grating fingers of the two structures as shown in **FIG. 7A**. However, that rotates the spot on the sample, and results in a signal even in the absence of any misalignment. The offset can be cancelled through calibration; however, this requires a target with larger footprint.

[**0042**] Another solution is to use a modified Wollaston prism **32'**, in which the optical axis **32***b'* (shown in a YZ plane as shown in **FIG. 7B**) in the first half of the prism is at +45° with respect to the length L of the prism **32'** and the optic axis **32***c'* (also shown in a YZ plane as shown in **FIG. 7B**) is at −45° to the length in the other half of prism **32'** on the other side of interface **32***a'* as shown in **FIG. 7B**. If the incoming beam **34** is vertically polarized (as indicated by line **34***c'* in **FIG. 7B**), it will be split by the prism into two substantially equal amplitude beams **34***a'*, **34***b'*, each at 45° polarization with respect to the fingers of the gratings **22**, **24** and giving substantially the same reflectance for substantially identical gratings. At the same time, the center line of the two spots will then be parallel to the fingers of the gratings as desired. Any residual difference in diffraction efficiencies of the two gratings can still be balanced by tuning the incoming polarization, using, for example, a half-wave plate.

[**0043**] Instead of having to move the Wollaston prism as described above, an alternative differential heterodyne system **100** requiring no moving parts is possible; this is illustrated in **FIG. 8A** as another embodiment. As shown in **FIG. 8A**, a coherent beam of radiation **102** is split into two beams **102***a* and **102***b* by polarizing beamsplitter **104**. Half wave plate **101** is employed to control the intensity ratio between E_1 and E_2 to compensate for the diffraction efficiency differences between the two overlay targets **22**, **24**. Beam **102***a* is frequency shifted upwards by modulator **106** by frequency ω_1 to become beam E_1 and beam **102***b* is frequency shifted upwards by a modulator **108** by frequency ω_2 to become beam E_2. The two modulated beams are reflected by mirrors **110** and passed through respective wave plates **112***a*, **112***b* so that E_1 and E_2 can pass through and be reflected respectively by the polarizing beam splitter **114**. The two beams pass through beamsplitter **116** to a birefringent element such as a Wollaston prism **32** which separates the two beams E_1 and E_2 on account of their different polarizations. Beam E_1 is collected by lens **36** towards structure **24** and beam E is collected by the lens towards structure **22**.

[**0044**] The +1 diffraction order $E_{1,+1}$ of beam E_1 from structure **24** is focused by lens **36** towards prism **32**. The +1 diffraction order $E_{2,+1}$ of beam E_2 from structure **22** is also focused by lens **36** and combined with the +1 diffraction order $E_{1,+1}$ by prism **32** into a single beam which is reflected by beamsplitter **116**. The polarizations of the fields $E_{1,+1}$, $E_{2,+1}$ are orthogonal to each other. Analyzer **118** is placed at substantially 45° to the polarization directions of $E_{1,+1}$, $E_{2,+1}$ so that the components passed by the analyzer have the same polarization and will interfere at detector **54**, after reflection by mirror **134**. Similarly, the −1 diffraction order signals $E_{1,-1}$, $E_{2,-1}$ of the respective beams E_1, E_2, by structures **24**, **22**, respectively, are focused by lens **36** towards the same spot in prism **32** which combines the two beams into a single beam $E_{1,-1}+E_{2,-1}$. Again the components of $E_{1,-1}$, $E_{2,-1}$ passed by the analyzer **118** have the same polarization and will interfere at detector **52**, after reflection by mirror **132**. The outputs of the detectors **52**, **54** are then provided to a phase detector **140** which detects a beat frequency ω_b which is equal to the difference between ω_1 and ω_2 in order to determine the misalignment or overlay target error Δx. The equations of the various optical signals E_1, E_2, $E_{1,+1}$, $E_{2,+1}$, $E_{1,-1}$, $E_{2,-1}$ are set forth below. In the equations below, $|E_1|$, $|E_2|$ are the amplitudes of the two beams E_1 and E_2 and ω_o is the frequency of input beam **102**. The terms θ_{n1} and θ_{n2} indicate the initial phase of input beam **102** and also the optical path length difference of the two beams between beamsplitter **104** and polarizing beamsplitter **114**. The terms ϕ_{+1}, ϕ_{-1}, ϕ_x, ϕ_z, and ϕ_w have the same meanings as those described above in the previous embodiment where the Wollaston prism is moved, and are set forth in equations (3)-(5) above.

$$E_1=|E_1|exp\{j(\omega_0 t+\omega_1 t+\theta_{n1})\} \quad (10)$$

$$E_2=|E_2|exp\{j(\omega_0 t+\omega_2 t+\theta_{n2})\} \quad (11)$$

$$E_{1,+1}=|E_1|\sqrt{\eta_{+1}{}^b}exp\{j(\omega_0 t+\omega_1 t+\theta_{n1}+\phi_{+1}{}^b+\phi_x)\} \quad (12)$$

$$E_{1,-1}=|E_1|\sqrt{\eta_{-1}{}^b}exp\{j(\omega_0 t+\omega_1 t+\theta_{n1}+\phi_{-1}{}^b-\phi_x)\} \quad (13)$$

$$E_{2,+1}=|E_2|\sqrt{\eta_{+1}{}^a}exp\{j(\omega_0 t+\omega_2 t+\theta_{n2}+\phi_{+1}{}^a+\phi_z+\phi_w)\} \quad (14)$$

$$E_{2,-1}=|E_2|\sqrt{\eta_{-1}{}^a}exp\{j(\omega_0 t+\omega_2 t+\theta_{n2}+\phi_{-1}{}^a+\phi_z+\phi_w)\} \quad (15)$$

[**0045**] The quantities $\sqrt{\eta_{+1}{}^b}$, $\sqrt{\eta_{+1}{}^a}$, $\sqrt{\eta_{-1}{}^b}$, $\sqrt{\eta_{-1}{}^a}$ are the diffraction efficiencies of the two structures for the +1 and −1 diffraction in the equations above. The output of detector **54** is given by equation (16) below and the output of detector **52** is given by equation 17 below.

$$S_{+1}\propto|E_{1,+1}+E_{2,+1}|^2=|E_1|^2\eta_{+1}{}^b+|E_2|^2\eta_{+1}{}^a+2|E_1||E_2| \sqrt{\eta_{+1}{}^a\eta_{+1}{}^b}\cos[\omega_b t+(\theta_{n2}-\theta_{n1})+(\phi_{+1}{}^a-\phi_{+1}{}^b)+\phi_z+\phi_w-\phi_x] \quad (16)$$

$$S_{-1}\propto|E_{1,-1}+E_{2,-1}|^2=|E_1|^2\eta_{-1}{}^b+|E_2|^2\eta_{-1}{}^a+2|E_1||E_2| \sqrt{\eta_{-1}{}^a\eta_{-1}{}^b}\cos[\omega_b t+(\theta_{n2}-\theta_{n1})+(\phi_{-1}{}^a-\phi_{-1}{}^b)+\phi_z+\phi_w-\phi_x] \quad (17)$$

[**0046**] S_{+1} and S_{-1} are sinusoidal functions at the beat frequency or difference frequency $\omega_b=\omega_1-\omega_2$ in the time domain. Again, where the two structures **22**, **24** are symmetric, the following phase relation would hold:

$$\phi_{+1}{}^a=\phi_{-1}{}^a$$
$$\phi_{+1}{}^b=\phi_{-1}{}^b \quad (18)$$

[**0047**] Thus, from equations (16)-(18) above, it is noted that the phase difference between S_{+1} and S_{-1}, is $2\phi_x$.

[**0048**] Therefore, by detecting the phase difference between the two detector outputs, the overlay target error Δx between the two structures **22**, **24** may be obtained from equations (3) and (9) above.

[**0049**] Advantageously, the detector **140** may be set to detect at the beat or difference frequency $\omega_1-\omega_2$ to improve the signal-to-noise ratio of ϕ_x.

[0050] From a comparison of **FIG. 8A** to **FIGS. 3A, 3B**, it will be evident-that the two diffracted and combined beams $E_{1,+1}+E_{2,+1}$ and $E_{1,-1}+E_{2,-1}$ as well as their corresponding detectors **54, 52** are not in the plane of the paper; instead, one combined beam and its corresponding detector are above the plane of the paper and the other combined beam and its corresponding detector are in the plane below the plane of the paper.

[0051] **FIG. 8B** is a partially schematic and partially cross-sectional view of a dual heterodyne differential phase metrology system for measuring misalignment of two adjacent overlay targets to illustrate another embodiment of the invention analogous to that in **FIG. 8A**. As shown in **FIG. 8B**, metrology system **100'** is similar to system **100** on **FIG. 8A**, except that anon-polarizing beamsplitter **114'** is used instead of the polarizing beamsplitter **114** of **FIG. 8A**. Waveplate **101** is again used for controlling the intensity in ratio between the two beams E, and E.

[0052] The typical heterodyne phase different ϕ_x detected is of the order of 10^{-4} radians where the spacing Λ of structures **22, 24** is of the order of 2 microns in equation (3) above. Therefore, with such or similar grating period of structures **22, 24**, it is possible to detect misalignment Ax which can be as small as 30 picometers.

[0053] **FIGS. 9A and 9C** illustrate another embodiment of the invention without any moving parts. **FIG. 9B** is a graphical plot of the output signals from the metrology system of **FIGS. 9A, 9C**. As shown in **FIGS. 9A, 9C**, a portion of an input coherent beam of radiation **102** at frequency ω_0 is reflected by mirror **202** and passes through an acoustooptic deflector (AOD) **204**. A portion **212** of the input beam at frequency ω_0 passes through the AOD without being deflected or changed in frequency and is collected by lens **36** towards structure **24**. Another portion **214** of the input beam **102** is upshifted by frequency ω and is deflected by the AOD **204** to provide an upshifted and deflected beam at frequency to $\omega_0+\omega$ which is also collected by lens **36** towards structure **22**.

[0054] Beam **214** is diffracted by structure **22** and the +1 and −1 orders of the diffraction are beams **214+** and **214−**, respectively. The two diffracted beams **214+** and **214−** are both at frequency $\omega_0+\omega$. The two diffracted beams **214+** and **214−** are collected by lens **36** towards AOD **204** which passes without deflection or change in frequency a portion thereof towards mirror **208**. The undeflected beam **212** at frequency ω_0 is diffracted by structure **24** into two diffracted beams **212+** and **212−**, both at frequency to ω_0. These two beams are collected by lens **36** towards the AOD **204** which deflects and downshifts in frequency by ω a portion of the two beams towards mirror **208**. The AOD **204** combines the deflected portion of beam **212+** and the undeflected portion of beam **214+** to form the +1 order mixed output signal S_{+1} so that the two portions would interfere and yield an output at beat frequency equal to 2ω. Similarly, AOD **204** would combine the deflected portion of beam **212−** and the undeflected portion of beam **214−** as the −1 order mixed signal output S_{-1} at beat frequency 2ω.

[0055] As in the previous embodiment shown in **FIGS. 8A, 8B**, any misalignment between the two structures **22, 24** in the X direction would introduce a phase difference ϕ_x between the +1 order (S_{+1}) and the −1 order (S_{-1}) of mixed outputs in **FIG. 9C**. Thus, equations 16-18 may then be used to derive the overlay target area Δ_x, where the beat frequency ω_b in equations 16 and 17 is equal to 2ω.

[0056] **FIG. 10** is a schematic view of the two structures **22, 24** illuminated by a single beam to illustrate another embodiment of the invention. Thus, instead of splitting single beam into two beams, for illuminating the two respective structures, a single beam may be used. **FIGS. 11A, 11B** are the front and side views of a system **300** employing a single beam for illuminating the two structures to illustrate yet another embodiment of the invention. As shown in **FIGS. 10, 11A, 11B**, this embodiment is analogous to that shown in **FIGS. 2, 3A** and 3B, except that a single beam **302** is employed that illuminates both structures **22, 24**. As shown in **FIGS. 10 and 11A**, the single beam **302** illuminates a portion of structure **22** and a portion of structure **24** at their edges next to each other. The +1 and −1 diffraction signals from the two structures are collected by lens **36** and combined and detected by two detectors (not shown) to provide the two outputs S_{+1} and S_{-1} as in the embodiment of **FIGS. 2, 3A** and 3B. A flow diagram illustrating the relative positions of the beams are shown in **FIG. 12**. As shown in **FIG. 12** the +1 diffraction beams from structures **22, 24** are combined into a single beam **340** and the −1 diffraction beams from the two structures are combined into a single beam **342**. The two beams are detected by respective detectors **52, 54** to provide the output S_{+1} and S_{-1} as before.

[0057] One consideration in the embodiment of **FIGS. 10, 11A, 11B** and **12** is that the alignment of the illuminating beam **302** is preferably controlled relative to the two structures to ensure that the relative intensity of the diffraction beams from both structures are held stable and substantially equal. This can be accomplished by precision beam positioning relative to the patterning on the wafer which can be augmented using an imaging system such as an optical microscope to visualize the beam location and make fine adjustments to the location of the beam **302**. Other methods include measuring the relative intensity of the diffraction components from the two structures in a feedback system to move the beam **302** to even and consistent alignment between the two structures. For such alignment, the wafer may be moved by means of cross-roller translation stages driven by micrometers. Alternatively, beam **302** may be moved by means of adjustable beam steering mirrors or galvanometer mirrors and the like. All such different alignment mechanisms are believed to be known to those skilled in the art.

[0058] In the embodiments described above, misalignment is detected along one direction, namely, the x direction. In order to discover misalignment along an orthogonal direction such as the y direction, typically a second optical detection system is employed. Yet another embodiment envisions a two-dimensional alignment system as illustrated in **FIG. 13**. For this purpose a pair of two-dimensional gratings C and D is created and positioned on their respective processing layers in the same manner as the previously described structures **22, 24**. In the case of a dual beam measurement configuration described above in reference to **FIGS. 2, 3A, 3B** and **4**, the two illumination beam on the two gratings would each give rise to four principal diffraction components, two in each axis of the gratings C and D.

[0059] Aside from the use of two-dimensional gratings C and D instead of one-dimensional gratings **22, 24**, and the

need to detect four outputs instead of two, the apparatus for the embodiment of **FIG. 13** is the same as the previous embodiment illustrated in reference to **FIGS. 2, 3A, 3B** and **4**. The two quartets of diffraction orders from gratings C and D are brought into alignment by the Wollaston prism **32** and four separate photodetectors **352, 354, 356** and **358** are used to separately measure the two sets of interference signals corresponding to the positive and negative diffraction orders in each of the two axes. Conveniently, the detector used in this configuration may be a quadrant photodiode. Interpretation of the phase information proceeds as before and alignment information in two axes may be simultaneously derived. The misalignment along the y direction is determined by calibration based on two targets on the same layer to offset the DC phase shift induced by the Wollaston prism for the diffraction in the y direction.

[**0060**] **FIG. 14** is a block diagram illustrating a lithographic instrument **400** in combination with a metrology system **100** for measuring misalignment of overlay targets to illustrate still another embodiment of the invention. As shown in **FIG. 14**, the misalignment between two overlay targets measured by the metrology system **100** of **FIG. 8A** may be supplied to lithographic instrument **400** for controlling a lithographic process, such as one performed by a lithographic stepper. Thus, the metrology system **100** may be integrated with instrument **400** to become an integrated system for the convenient operation of misalignment detection and lithographic process control. Alternatively misalignment information may be used to determine probable device yield, and to make decision about future processing or rework of the devices. The process for performing such yield analysis and management is known to those skilled in the art so that no details need to be provided herein. This can also be done by supplying the misalignment of overlay targets information to instrument **400**, where the instrument is equipped with yield analysis and management capability residing in a microprocessor in the instrument **400**, in addition to lithographic control. Alternatively, such capability may reside in processing device or processor **50**.

[**0061**] While the invention has been described above by reference to various embodiments, it will be understood that changes and modifications may be made without departing from the scope of the invention, which is to be defined only by the appended claims and their-equivalents.

1. A method for detecting misalignment of two periodic structures placed next to each other so that they are periodic substantially along a first line, comprising:

illuminating a portion of each of the two structures using radiation that is substantially coherent, each of said portions having a dimension along the first line larger than the period of the corresponding structure;

detecting diffracted radiation signals from the illuminated portions of the structures to provide at least one output signal; and

determining from the at least one output signal a misalignment between the structures.

2-43. (canceled)

* * * * *